J Low Temp Phys (2016) 182:61–71
DOI 10.1007/s10909-015-1353-3

Crystalline, Magnetic and Electronic Structure of the Ba_2DySbO_6 Complex Perovskite

R. Cardona[1] · R. Moreno Mendoza[1] · L. A. Carrero Bermúdez[1] · D. A. Landínez Téllez[1] · J. Roa-Rojas[1]

Received: 1 September 2015 / Accepted: 19 October 2015 / Published online: 6 November 2015

Abstract In this work, we report the synthesis of the Ba_2DySbO_6 new double perovskite by means of the solid-state reaction recipe from high-purity oxide powders of $BaCO_3$, Dy_2O_3, and Sb_2O_5. The analysis of the crystal structure was carried out through the X-ray diffraction technique with posterior Rietveld refinement of the experimental diffraction data by the GSAS code. Results reveal that the Ba_2DySbO_6 material crystallizes in a rhombohedral perovskite structure, belonging to the *R-3 (#148)* space group with lattice parameter $a = 5.96260(5)$ Å, and angle $\alpha = 60.008°$. The magnetic characterization was performed by measurements of magnetic susceptibility as a function of temperature. The behavior observed in the temperature regime from 4 K up to 300 K was paramagnetic. The characteristic magnetic parameters were obtained from the fitting with the Curie equation, obtaining the values of susceptibility independent of temperature 0.00633 emu/mol and effective magnetic moment 8.9 μ_B, which is 84 % in agreement with the expected value predicted by the Hund's rules. The electronic structure was calculated by means of linearized augmented plane waves in the framework of the density functional theory (DFT). This study considers the cohesion energies as a function of the lattice parameter, with a lattice constant a, whose value is 98 % in agreement with the experimental result. Curves of density of states as a function of the wave number reveal that this material behaves as an insulator with energy gap 3.65 eV. This result was corroborated by diffuse reflectance experiments adjusted to the Kubelka–Munk equation. The effective magnetic moment obtained from the DFT calculations was 7.7 μ_B.

✉ J. Roa-Rojas
jroar@unal.edu.co

[1] Grupo de Física de Nuevos Materiales, Departamento de Física, Universidad Nacional de Colombia, AA 5997 Bogotá DC, Colombia

Keywords Complex perovskite · Crystalline structure · Magnetic behavior · Electronic structure

1 Introduction

Ceramic materials represent a great percentage of systems which are actually investigated by the physics and chemistry of solids. Particularly, the perovskite family has concentrated important attention in the last decades. From the point of view of chemical composition, perovskites have been characterized by the ideal formula ABX_3, where A generally is an alkaline earth element, B represents a transition metal or rare earth element, and X, more of times, is the oxygen [1]. Modifications of atomic radii of A and B, introduce structural distortions and new crystalline phases. Inclusions of rare earth elements give the possibility to produce materials with exotic electric and magnetic properties [2,3]. Partial substitutions of the A and B cations give rise to complex materials as the double perovskites $A_2BB'O_6$ [4]. Its chemical configuration supplies multiple chances to combine different elements, generating the possibility to synthesize new materials, which involve a great variety of physical properties. Depending on magnetic and electric characteristics of B and B′ it is relatively easy to create new perovskite systems with half-metallic properties [5], magnetoelectric response [6], or magnetic ordering [7], which offer promissory perspectives in the new spintronics technology [8]. In recent years, Sb-based double perovskites have been synthesized and studied due to their dielectric properties [9,10], nanostructure [11], and nanoparticles [12], among others. In this paper we propose the synthesis and characterization of Ba_2DySbO_6 ceramic material. We describe the crystalline structure of this double perovskite and perform morphological, magnetic, and electronic analyses. Furthermore, we present results of measurements of the magnetic response as a function of temperature. Moreover, considering that in recent years the density functional theory (DFT) has constituted in a strong tool to study electronic properties in perovskite-like material [13], we carried out a study of the electronic properties of these materials, in order to establish the type of hybridization between the orbitals of DyO_6 and SbO_6 octahedra present in the structure. This calculation is the greatest motivation of this work and the experimental corroboration of the theoretical predictions with regard to the energy gap. Furthermore, a thorough analysis of the crystal structure for this material has not been reported.

2 Experimental Setup

Samples were synthesized through the standard solid-state reaction recipe. Precursor powders of Dy_2O_3, Sb_2O_5, and Ba_2CO_3 (Aldrich 99.9%) were stoichiometrically mixed according to the chemical formula Ba_2DySbO_6. The mixture was ground to form a pellet and annealed at 1000 °C for 30 h. The samples were then regrinded, repelletized, and sintered at 1100 °C for 40 h and 1200 °C for 40 h. X-ray diffraction (XRD) experiments were performed by means of a PW1710 diffractometer with $\lambda_{CuK\alpha}$ = 1.54064 Å. Rietveld refinement of the diffraction patterns was carried out by the GSAS program [14]. Morphological studies were performed by means of scanning

electron microscopy (SEM) experiments through the utilization of VEGA 3 equipment. Field cooling measurements of the magnetic susceptibility as a function of temperature were carried out by using an MPMS Quantum Design SQUID. Diffuse reflectance experiments were performed by using a VARIAN Cary 5000 UV–Vis–NIR spectrophotometer, which has an integration sphere with a PMT/Pbs detector.

3 Theoretical Calculations

In order to determine the electronic and band structures we applied the full-potential linear augmented plane wave method (FP-LAPW) within the framework of the Kohn–Sham DFT [15], and adopted the generalized gradient (GGA) approximation for the exchange-correlation energy due to Perdew et al. [16]. The self-consistent process is developed by the numeric package Wien2k [15]. Taking the experimental unit cell data as input, the structure studied in this work were fully relaxed with respect to their lattice parameters and the internal degrees of freedom compatible with the space group symmetry of the crystal structure. The resulting energies versus volume functions have been fitted to the equation of state due to Murnaghan [17] in order to obtain the minimum energy value, the bulk modulus, its pressure derivative and the equilibrium lattice parameters, and associated volume. The muffin-tin radiuses used for Ba_2DySbO_6 were 2.20; 2.50; 2.12; and 1.82 for Ba, Dy, Sb, and O, respectively, angular momentum up to $l = 10$ inside the muffin-tin sphere, a maximum vector in the reciprocal space of $Gmáx = 12.0$, RMT*K_{max}=7.0, and a mesh of 1000 points in the first Brillouin zone (equivalent to a maximum of 250 k points in the irreducible Brillouin zone). Finally, the convergence criterion for the self-consistent calculation was 0.0001 Ry for the total energies, 0.0001 Bohr in the charge and 1.0 mRy/u.a. in the internal forces. Spin polarization was included in the calculations.

4 Results and Discussion

Figure 1 shows the XRD patterns obtained for Ba_2DySbO_6. In the picture, black symbols represent the experimental data and the line corresponds to simulated pattern by means of GSAS code. Base line is the difference between theoretical and experimental results. Refinement parameters of Fig. 1 were $x^2 = 1.613$ and $R_{(F2)} = 6.04\,\%$. This refinement is acceptable, considering that a good refinement is expected for parameters $x^2 < 1.7$ and $R_{(F2)} < 10\,\%$. From the Rietveld refinement it was established that these materials crystallize in a rhombohedral perovskite structure, space group *R-3 (#148)*. The structural parameter obtained from the refinement was $a = 5.96260(5)$ Å with trigonal angle $\alpha = 59.9862°$ and tilt angle $\beta = -8.6002°$. These results are 99.2 % in agreement with the theoretical values obtained from the Structure Prediction Diagnostic Software SPuDs [18], which predicts $a = 6.0091$ Å and $\alpha = 59.4417°$.

In these ceramic materials the explanation of distortion from the ideal cubic perovskite structure is clear because the double perovskite have the generic formula $A_2BB'O_6$, and for this type of material the tolerance factor τ, is calculated by the ratio $\tau = \frac{r_A + r_O}{\sqrt{2}(\frac{r_B + r_{B'}}{2} + r_O)}$, where r_A, r_B, $r_{B'}$, and r_O are the ionic radii of the A, B, B', and O

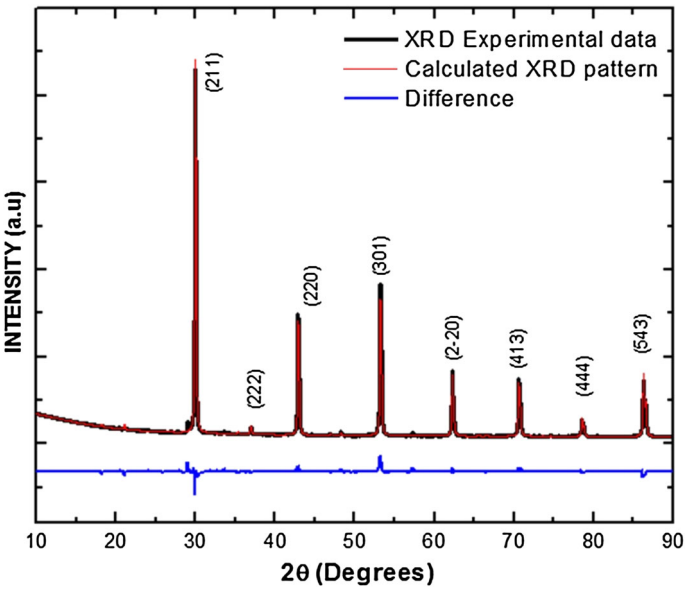

Fig. 1 Characteristic XRD pattern for the Ba_2DySbO_6 double perovskite. *Black symbols* represent experimental diffraction data, *continuous lines* are the simulated patterns, and *base line* is the difference between experimental and calculated values (Color figure online)

Table 1 Atomic positions of cations and anions on the unit cell for Ba_2DySbO_6

Atom	Wyckoff Site	x	y	z
Ba	2*c*	0.250000	0.250000	0.250000
Dy	1*a*	0.000000	0.000000	0.000000
Sb	1*a*	0.500000	0.500000	0.500000
O1	6*f*	−0.223282	−0.278818	0.285163

ions, respectively. If τ is equal to unity, there is ideal cubic perovskite structure, and if $\tau < 1$ the structure is distorted from the cubic symmetry. The value of tolerance factor obtained for the Ba_2DySbO_6 complex perovskite was 0.9771. The Wyckoff positions obtained from the refinement analysis are presented in Table 1.

The corresponding structure of the Ba_2DySbO_6 material is showed in Fig. 2. In the picture, it is observed that the DyO_6 and SbO_6 octahedra have not the same directions. As showed in Fig. 2a and b, there is a difference between directions of the DyO_6 and SbO_6 octahedra. The most important has to do with the nature of the rhombohedral structure, since the trigonal angle $\alpha = 59.4417°$ is quite far from 90° degrees corresponding to the ideal cubic cell. Furthermore, the tilt of the DyO_6 and SbO_6 octahedra occurs out of phase for an angle $\beta = -8.5850°$, corresponding to the Glazer notation $a-a-a-$, whose symmetry involves reflections, signaling odd–odd–odd reflections, which is characterized by cationic ordering and simple octahedral tilting [19].

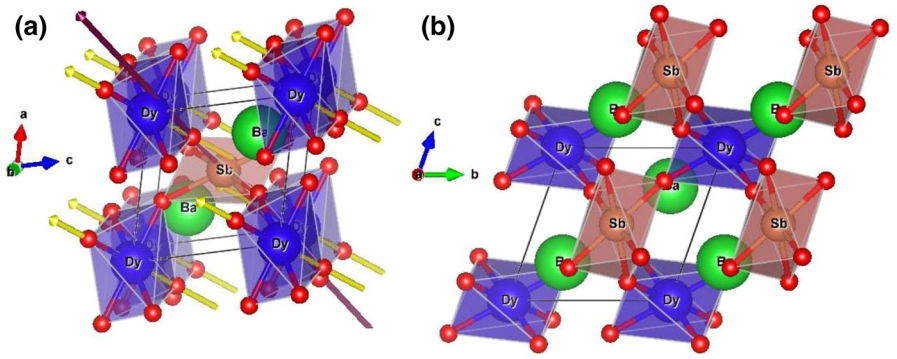

Fig. 2 Rhombohedral structure of the Ba_2DySbO_6 complex perovskite, **a** ca-plane and **b** bc-plane (Color figure online)

The structural distortions as tilting or rotation of the BO_6 and $B'O_6$ octahedra in $A_2BB'O_6$ double perovskites, with B or B′ magnetic cation, are usually responsible for changes in the magnetic response such as irreversibility, frustration, and decrease in value of the effective magnetic moment [20].

SEM images of the material shown in Fig. 3 reveal a qualitative approximation to the surface microstructure. Picture (a) evidences the formation of clusters of polyhedral grains and interstitial particulate grains. From picture (b) it is clear that the grains could end up having a few tens of nanometer, forming groups which have appearance of clusters of several micrometer sizes.

By applying the EDX microprobe of the VEGA3 TESCAN microscope, the percentages of the constituent elements of the material were obtained, as reported in Table 2.

The values in Table 2 confirm that the material does not contain other elements than those corresponding to the expected stoichiometry Ba_2DySbO_6. However, the experimental result reveals an apparent low content of the oxygen anion against an increase in the percentage of Ba, Dy, and Sb cations, which may be because the resolution of the device is slightly affected because oxygen is a very light element compared to the other constituents of the compound.

Measurements of magnetic susceptibility as a function of temperature on the application of $H = 50$ Oe reveal the paramagnetic character of the Ba_2DySbO_6 complex perovskite. Figure 4 shows the Curie fitting performed following the equation $\chi = \chi_0 + (C/T)$.

In the Curie equation, $C = N\mu_{\text{eff}}^2/(3K_B)$ is the Curie constant, N is Avogadro's number, μ_{eff} is the effective magnetic moment ($\mu_{\text{eff}} = P_{\text{eff}}\mu_B$), P_{eff} represents the effective Bohr magneton number, μ_B is the Bohr magneton, K_B is the Boltzmann constant, and $\mu_0 = 0.00329$ emu/mol is the temperature-independent susceptibility term. From the Curie constant C the effective magnetic moments for Ba_2DySbO_6 material was calculated to be $8.9\,\mu_B$. This value is 84 % in agreement with the theoretical expected moments obtained from the Hund's rules [21]. The difference is attributed to other magnetic effects due to the hybridization of the *d-Sb* and *f-Dy* orbital and non-preferential spin orientations in the DyO_6 and SbO_6 octahedra due to structural

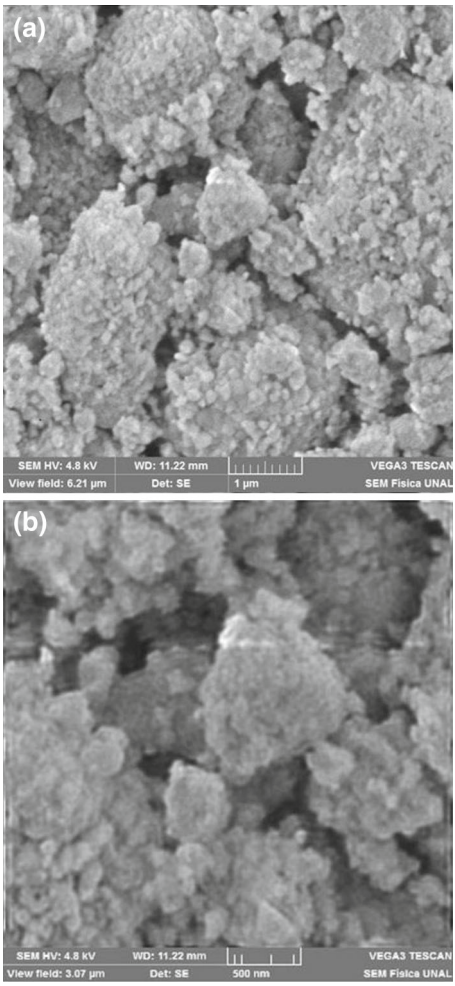

Fig. 3 Granular topology of the surface obtained from SEM images for the Ba_2DySbO_6 perovskite-like material

Table 2 Compositional percentages of elements for Ba_2DySbO_6 obtained from EDX

Element	Theoretical %	Experimental %
Ba	41.93	42.85
Gd	24.82	25.13
Sb	18.59	19.01
O	14.66	13.01

distortions. Furthermore, the slightly greater curvature of the fitting with respect to the experimental data may have caused this difference. In the inset of Fig. 4, in which the absolutely linear behavior of inverse susceptibility as a function of temperature is illustrated, the purely paramagnetic character of the material is clearly observed. The extrapolating $1/\chi$ on the temperature axis falls in $T = 0$ K.

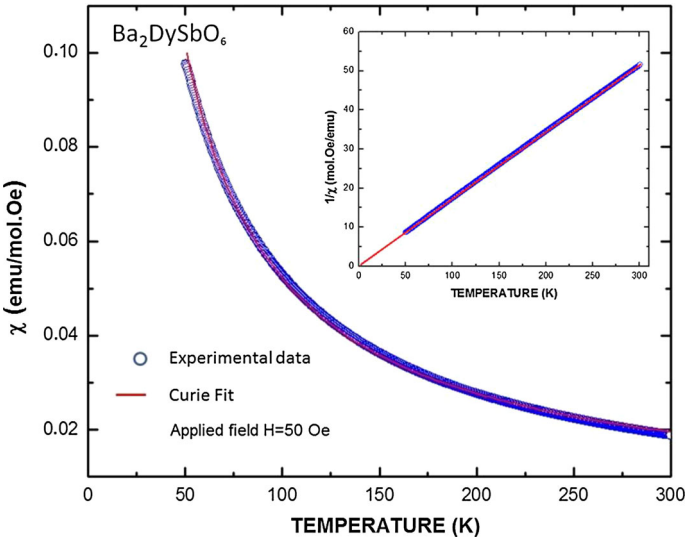

Fig. 4 Magnetic behavior of Ba_2DySbO_6 material obtained from measurements of susceptibility as a function of temperature. *Red line* corresponds to the fitting with the Curie equation (Color figure online)

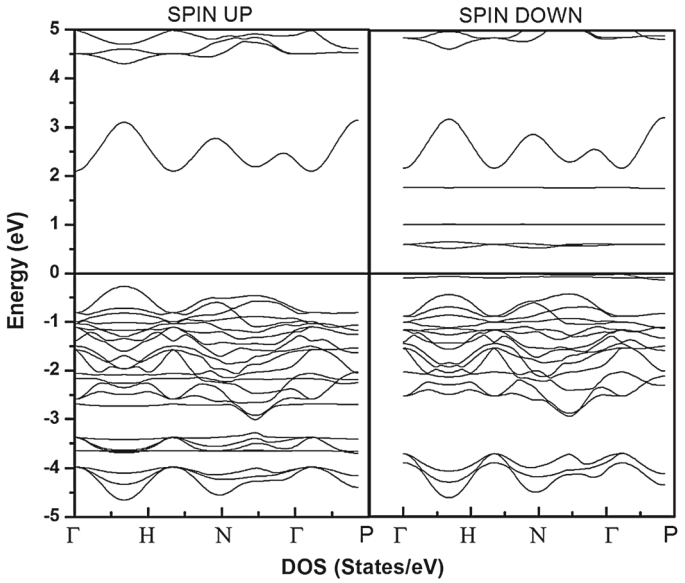

Fig. 5 Spin-polarized band structure calculated for the Ba_2DySbO_6 double perovskite

Figure 5 shows the band structure for both up- and down-spin polarizations, i.e., the spin-up and spin-down occupation of the valence electrons in the energy levels that characterize them. In the picture, $E = 0$ eV corresponds to the Fermi level. It is observed that these materials evidence indirect semiconductor behavior with gap energy through the Fermi level from -0.25 eV up to 2.2 eV (width 2.45 eV) for the

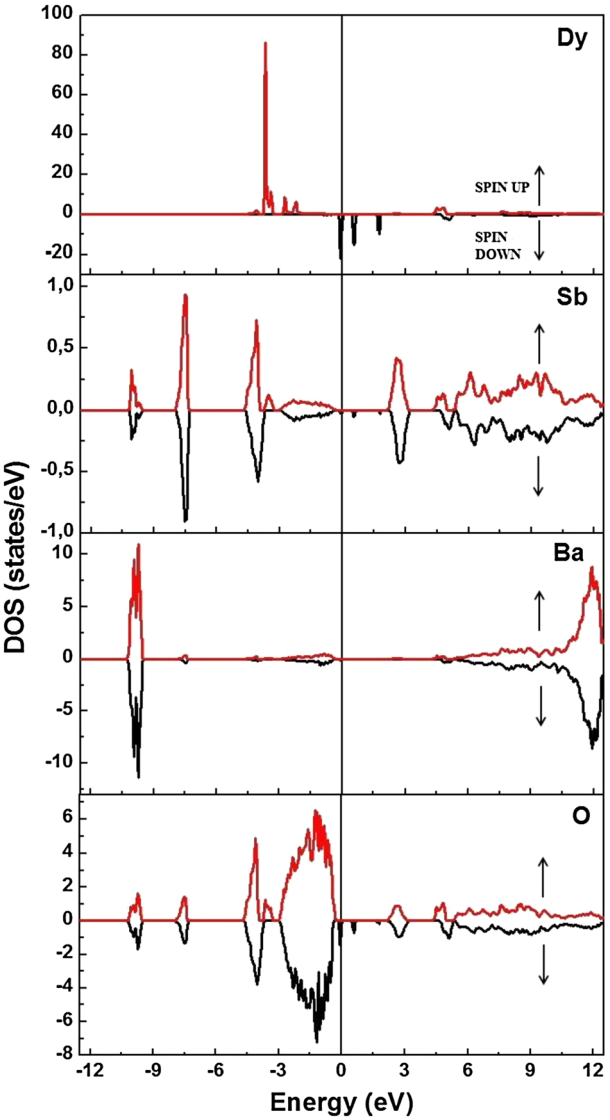

Fig. 6 Partial DOS with spin-up and -down polarizations for the Ba_2DySbO_6 double perovskite (Color figure online)

spin-up polarization and between −0.02 and 0.53 eV (width 0.55 eV) for the spin-down orientation.

The partial densities of states (DOS) for the Ba_2DySbO_6complex perovskite are exemplified in Fig. 6. As in Fig. 5, the energy zero corresponds to the Fermi level reference. It is important to elucidate that close the Fermi level there are contributions due to the *O-2p* hybridizations but *Dy-4f* spin-up orbitals are responsible for priority contributions. Very incipient contributions of *Sb-3d* states are observed. This behavior

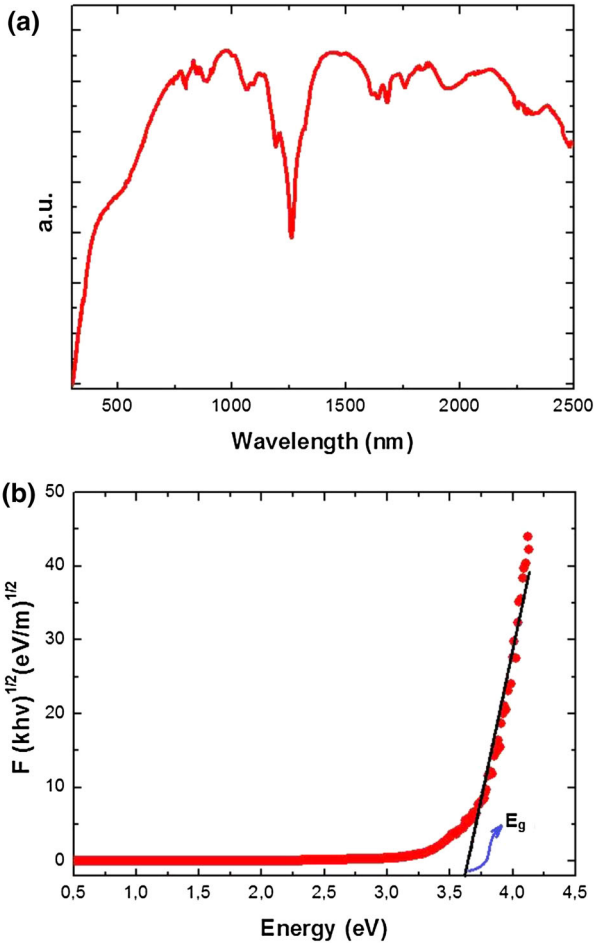

Fig. 7 **a** Diffuse reflectance results for the Ba_2DySbO_6 material. **b** Kubelka–Munk fitting (Color figure online)

can be clearly seen in Figs. 5 and 6 in the energy range between −8.72 and −0.05 eV. Localized states attributed to *Sb-3d, Ba-6s*, and *O-2p* appear far the Fermi level, below −9.00 eV. On the other hand, in the conduction band, it is observed in Figs. 5 and 6 that available states are majority due to the *Dy-4f* spin-down orbitals with very small contributions of the *Sb-3d* and *O-2p* spin-up and -down levels.

The magnetic moment of mixed charge density was calculated to be 7.7 μ_B for Ba_2DySbO_6. This value is relatively different from the value obtained experimentally. However, an important element to be taken into account has to do with the clutter of *Dy* and *Sb* cations in the structure of the double perovskite, which can not only distort octahedra but also modify the magnetic response of the material.

Results of diffuse reflectance experiments are shown in Fig. 7. Reflectance values were acquired at 1 nm intervals over the 300–2500 nm, as shown in Fig. 7a. The absorption of UV–Vis–NIR radiation reveals that the molecules of the Ba_2DySbO_6 material

cause the excitation of electrons from the ground state to exited state which produces electronic jumps between quantum levels. The quantum characteristics energy, which depends on the electronic configuration, is calculated from the radiated energy. By applying the Kubelta–Munk model, currently used to the measurement of the band gap in powder samples, the respective band gap for the Ba_2DySbO_6 perovskite is obtained as showed in Fig. 7b. It is observed in the picture that a spontaneous absorption appears for a wavelength of 1266 nm, which generally is attributed to structural defects or vacancies. From the adjustment to the Kubelka–Munk equation it was determined that the energy gap of the Ba_2DySbO_6 is 3.65 eV, which is significantly greater than the theoretic prediction given by the DOS calculations. It is important to note that the cause of this difference may be related to the exchange-correlation potential used in the calculations.

5 Conclusions

The Ba_2DySbO_6 complex has been synthesized by the solid-state reaction procedure. A study of the crystalline and electronic structure was performed through the FP-LAPW into the framework of the DFT. The results reveal that a rhombohedral perovskite is the more stable structure with a lattice parameter 5.96260(5) Å. Close to the Fermi level an energy gap of 2.45 eV was observed for the spin-up polarization and 0.55 eV for the other, which permitted to classify this material as semiconductor. The largest contribution to the effective magnetic moment, due to the Dy^{3+} cations, evidenced a value of 7.7 μ_B. The crystalline structure was experimentally determined by means of measurements in a Panalytical XPert Pro XRD with a Rietveld refinement of the diffraction pattern through de GSAS code. Results are 99.2 % in agreement with those theoretically predicted. Measurements of magnetic susceptibility as a function of temperature reveal the paramagnetic feature of this material. From the fitting with the Curie law the effective magnetic moment was obtained to be 8.9 μ_B, which is slightly higher that the theoretical value for the Dy^{3+} isolated cation predicted by $\mu_{\text{eff}} = g\sqrt{J(J+1)}$, where g represents the Landé's factor and J is the quantic number related to the $4f$ electronic orbital. Experiments of diffuse reflectance and fittings with the Kubelka–Munk equation permitted to obtain an energy gap of 3.65 eV, which is slightly greater than the theoretical value predicted by DFT because the exchange-correlation potential utilized for our calculations.

Acknowledgments This work was partially financed by DIB (National Uinversity of Colombia—Bogotá).

References

1. R.M. Hazen, Sci. Am. **258**, 54 (1988)
2. P.A. Sharma, J.S. Ahn, N. Hur, S. Park, S.B. Kim, S. Lee, J.G. Park, S. Guha, S.W. Cheong, Phys. Rev. Lett. **93**, 177202 (2004)
3. X. Lu, J. Xie, H. Shu, J. Liu, C. Yin, J. Lin, Mater. Sci. Eng. B **138**, 289 (2007)
4. C.A. Triana, D.A. Landínez Téllez, J. Arbey Rodríguez, F. Fajardo, J. Roa-Rojas, Mater. Lett. **82**, 116 (2012)

5. M. Bonilla, D.A. Landínez, J. Arbey Rodríguez, J. Albino Aguiar, J. Roa-Rojas, J. Magn. Magn. Mater. **320**, e397 (2008)
6. V.R. Palkar, S.K. Malik, Solid Stat. Commun. **134**, 783 (2005)
7. S.E. Lofland, T. Scabarozi, Y. Moritomo, Sh Xu, J. Magn. Magn. Mater. **260**, 181 (2003)
8. A. Di Trolio, R. Larciprete, A.M. Testa, D. Fiorani, P. Imperatori, S. Turchini, N. Zema, J. Appl. Phys. **100**, 13907 (2006)
9. C. Barthi, T.P. Sinha, Solid Stat. Sci. **12**, 498 (2010)
10. A. Dutta, T.P. Sinha, Int. J. Mod. Phys. B **21**, 2965 (2007)
11. C. Vijayakumar, H.P. Kumar, S. Solomon, J.K. Thomas, P.R.S. Warriar, J. Koshy, Bull. Mater. Sci. **31**, 719 (2008)
12. C. Vijayakumar, S.U.K. Nair, P.R.S. Wariar, J. Koshy, S. Solomon, H.P. Kumar, J.K. Thomas, Modern Phys. Lett. B **21**, 1227 (2007)
13. R. Cardona, D.A. Landínez, M. Arbey Rodríguez, F. Fajardo, J. Roa-Rojas, J. Magn. Magn. Mater. **320**, e85 (2008)
14. A.C. Larson, R.B. Von Dreele, in *General Structure Analysis System (GSAS)* (Los Alamos National Laboratory Report LAUR, 2000) pp. 86–748
15. P. Blaha, K. Schwarz, G.K.H. Madsen, D. Kvasnicka, J. Luitz, *WIEN2k, an Augmented Plane Wave + Local Orbitals Program for Calculating Crystal Properties* (Karlheinz Schwarz Techn. Universität Wien, Vienna, 2001)
16. J.P. Perdew, S. Burke, M. Ernzerhof, Phys. Rev. Lett. **77**, 3865 (1996)
17. F.D. Murnaghan, Proc. Natl. Acad. Sci. USA **30**, 244 (1944)
18. M.W. Lufaso, P.M. Woodward, Acta Crystallogr. B **57**, 725 (2001)
19. A.M. Glazer, Acta Crystallogr. A **31**, 756 (1974)
20. M.L. Medarde, J. Phys. Condens. Mater. **9**, 1679 (1997)
21. B.D. Cullity, C.D. Graham, *Introduction to Magnetic Materials*, 2nd edn. (IEEE Press, Hoboken, 2009)